

Momentum space anisotropy in doped Mott insulators

Tiago C. Ribeiro

Department of Physics, Massachusetts Institute of Technology, Cambridge, Massachusetts 02139, USA

(Dated: October 7, 2017)

We study the single hole $tt't''J$ -model numerically to address the momentum space anisotropy found in doped Mott insulators. A simple two band picture to understand how the doped hole is screened by the spin background in states of different momenta is proposed. In this picture, the disparity between the nodal and antinodal regions, observed by experiments in the underdoped cuprate superconductors, follows from local energetic considerations and amounts to the distinction between well defined quasiparticle behavior and spin-charge separation related phenomenology.

Introduction - It is known, both experimentally and theoretically, that doped Mott insulators can be significantly anisotropic in momentum space. Explaining this behavior is relevant to understanding the properties of metals close to the Mott insulating state, like the pseudogap regime in high- T_c superconductors. [1, 2]

The pseudogap measured by ARPES is the energy difference between the one-electron spectral features at the nodal [$\vec{k} = (\pm\frac{\pi}{2}, \pm\frac{\pi}{2})$] and antinodal points [$\vec{k} = (\pi, 0), (0, \pi)$]. [3] This difference, which increases as both the temperature and the level of doping in the CuO_2 layers are reduced, is accompanied by the anisotropic behavior in k -space present in various experimental observations. [2, 3, 4, 5, 6, 7, 8, 9] Indeed, the deeply hole underdoped regime shows a clear nodal-antinodal dichotomy as low energy quasiparticle peaks exist around the nodes while there is no evidence of quasiparticle-like behavior near the antinodal points. [2, 4, 5] In electron underdoped cuprates, low energy spectral weight appears around $(\pi, 0)$ instead as the pseudogap is pushed toward the zone diagonal. [10] Interestingly, Raman spectroscopy [11] and the violation of the Wiedemann-Franz law [12] in electron doped materials suggests the presence of chargeless excitations around $(\frac{\pi}{2}, \frac{\pi}{2})$. Hence, the pseudogap in the one-particle dispersion appears to strongly reduce the electronic character of excitations in the pseudogap region.

Strongly correlated materials close to the Mott insulator transition are notorious for the near degeneracy of different ordered states, some of which have been argued to provide a scattering mechanism that reduces quasiparticle features in the pseudogap region. [2, 7, 13, 14] In this letter, we propose a different scenario to understand the observed momentum space anisotropy. In particular, we argue that states close to $(\frac{\pi}{2}, \frac{\pi}{2})$ and $(\pi, 0)$ are different because, due to the competition between the spin exchange energy and the hole kinetic energy, spins surrounding the hole in states near $(\frac{\pi}{2}, \frac{\pi}{2})$ behave differently from the spins surrounding the hole in antinodal states. [15, 16] The nodal-antinodal dichotomy then reflects the existence of two distinct ways in which the lattice spins screen the doped holes.

The 2D $tt't''J$ -model, which is the simplest model to study doped Mott insulators as of relevance to the

cuprate systems, reproduces the experimental pseudogap dispersion and accounts for anisotropic behavior in k -space. [15, 16, 17, 18, 19] Below, we employ the exact diagonalization (ED) and the self-consistent Born approximation (SCBA) techniques to study the single hole $tt't''J$ -model and to address how the hole is screened by the local spins in different regions of momentum space. We find that the single hole states can be understood as the superposition of two distinct states, namely a hole-like quasiparticle state and a state where the hole strongly distorts the surrounding spins. Due to their different properties, these states predominate in different parts of k -space in the pseudogap regime, thus leading to the disparity between the nodal and antinodal regions. Our results are valid for both hole and electron doped materials – for our purposes, the main distinction between the two regimes is that in the former the pseudogap opens in the antinodal region while in the latter it opens in the nodal region.

Model - The single hole 2D $tt't''J$ Hamiltonian is

$$H_{tt't''J} = - \sum_{\langle ij \rangle, \sigma} t_{ij} \left(\tilde{c}_{i,\sigma}^\dagger \tilde{c}_{j,\sigma} + H.c. \right) + \sum_{\langle ij \rangle} J_{ij} \mathbf{S}_i \cdot \mathbf{S}_j \quad (1)$$

where t_{ij} equals t , t' and t'' for first, second and third nearest neighbor sites respectively and vanishes otherwise. $\tilde{c}_{i,\sigma}$ is the constrained operator $\tilde{c}_{i,\sigma} = c_{i,\sigma}(1 - n_{i,-\sigma})$. The exchange interaction only involves nearest neighbor spins for which $J_{ij} = J$. We only consider $0.2 < J < 0.8$ (units are set so that $t = 1$). Unless otherwise stated, all our results come from the ED of $H_{tt't''J}$ on a 4×4 lattice. Since we want to analyze how the hole affects the local configuration of the surrounding spins we believe that the study of such a small lattice is relevant. We also present results from the SCBA approach to the tJ model [20, 21, 22] on a 16×16 lattice to further support the ED analysis.

We start by considering the $t', t'' = 0$ case. In particular, we use the ED technique to determine the lowest energy state for each momentum, denoted by $|\psi_{\mathbf{k}}, J\rangle$, for both $J = 0.2$ and $J = 0.6$. Quite surprisingly, we find that if we perform the same calculation for different values of J the resulting states $|\psi_{\mathbf{k}}, J\rangle$ have almost complete overlap with the Hilbert space $\{|\psi_{\mathbf{k}}, J = 0.2\rangle, |\psi_{\mathbf{k}}, J =$

J	0.3	0.4	0.5	0.6	0.7	0.8	
$(\frac{\pi}{2}, \frac{\pi}{2})$	0.9994	0.9994	0.9998	1	0.9998	0.9990	
$t' = 0$	$(\pi, 0)$	0.9994	0.9994	0.9998	1	0.9998	0.9990
$t'' = 0$	$(\pi, \frac{\pi}{2})$	0.9972	0.9977	0.9993	1	0.9992	0.9970
ED	$(\frac{\pi}{2}, 0)$	0.9975	0.9980	0.9994	1	0.9994	0.9977
	$(0, 0)$	0.9946	0.9923	0.9963	1	0.9938	0.9766
$(\frac{\pi}{2}, \frac{\pi}{2})$	0.9996	0.9996	0.9998	1	0.9998	0.9990	
$t' = 0$	$(\pi, 0)$	0.9994	0.9994	0.9998	1	0.9997	0.9986
$t'' = 0$	$(\pi, \frac{\pi}{2})$	0.9989	0.9988	0.9996	1	0.9995	0.9978
SCBA	$(\frac{\pi}{2}, 0)$	0.9989	0.9988	0.9996	1	0.9995	0.9978
	$(0, 0)$	0.9016	0.9005	0.9766	1	0.9842	0.9488
$(\frac{\pi}{2}, \frac{\pi}{2})$	0.9994	0.9994	0.9998	1	0.9998	0.9990	
$t' = -0.2$	$(\pi, 0)$	-	1	0.9998	0.9997	0.9999	1
$t'' = 0.1$	$(\pi, \frac{\pi}{2})$	0.9936	0.9952	0.9986	1	0.9987	0.9950
ED	$(\frac{\pi}{2}, 0)$	0.9907	0.9943	0.9986	1	0.9988	0.9957
	$(0, 0)$	0.9880	0.9856	0.9943	1	0.9940	0.9807

TABLE I: Square of the overlap of $|\psi_{\mathbf{k}}, J, t', t''\rangle$ with the Hilbert space $\{|\psi_{\mathbf{k}}, J = 0.2, t', t''\rangle, |\psi_{\mathbf{k}}, J = 0.6, t', t''\rangle\}$ for different J and \mathbf{k} . Both ED and SCBA results are shown for $t', t'' = 0$. ED results are also shown for $t' = -0.2, t'' = 0.1$. For $t' = -0.2, t'' = 0.1$ and $\mathbf{k} = (\pi, 0)$ the Hilbert space $\{|\psi_{\mathbf{k}}, J = 0.4, t', t''\rangle, |\psi_{\mathbf{k}}, J = 0.8, t', t''\rangle\}$ was used instead.

0.6)} (Table I). The SCBA technique leads to the same conclusion (Table I), thus supporting that this result is not specific to the 4×4 lattice used in the ED calculation.

Therefore, for $0.2 < J < 0.8$, the wave function $|\psi_{\mathbf{k}}, J\rangle$ can be written approximately as $|\psi_{\mathbf{k}}, J\rangle \cong q(J)|Q_{\mathbf{k}}\rangle + u(J)|U_{\mathbf{k}}\rangle$. Here, $q(J)$ and $u(J)$ are J -dependent coefficients obeying the normalization condition $q(J)^2 + u(J)^2 = 1$. $|Q_{\mathbf{k}}\rangle$ and $|U_{\mathbf{k}}\rangle$ are orthonormal states that span the 2D Hilbert space $\{|\psi_{\mathbf{k}}, J = 0.2\rangle, |\psi_{\mathbf{k}}, J = 0.6\rangle\}$. Of course, there is freedom in choosing $|Q_{\mathbf{k}}\rangle$ and $|U_{\mathbf{k}}\rangle$. A physically sensible choice, though, comes from requiring that $q(J)$ increases with J while $u(J)$ decreases. Since increasing J enhances the quasiparticle features of doped carriers, [20] this is automatically satisfied if the quasiparticle spectral weight vanishes for $|U_{\mathbf{k}}\rangle$, *i.e.* $\langle U_{\mathbf{k}} | \tilde{c}_{\mathbf{k}, \sigma} | \text{HF GS} \rangle = 0$ where $|\text{HF GS}\rangle$ is the groundstate of the half filled system. This prescription uniquely determines Q states ($|Q_{\mathbf{k}}\rangle$) and U states ($|U_{\mathbf{k}}\rangle$), [23] which are not eigenstates of $H_{tt't''J}$, as long as $\langle \psi_{\mathbf{k}}, J | \tilde{c}_{\mathbf{k}, \sigma} | \text{HF GS} \rangle \neq 0$.

For general \mathbf{k} and t', t'' the state $|\psi_{\mathbf{k}}, J, t', t''\rangle$ only has non-zero quasiparticle spectral weight for J larger than a certain $J_c(\mathbf{k}, t', t'')$. The above prescription can be applied for $J > J_c(\mathbf{k}, t', t'')$, in which case it is a good approximation to write $|\psi_{\mathbf{k}}, J, t', t''\rangle \cong q(J, t', t'')|Q_{\mathbf{k}}, t', t''\rangle + u(J, t', t'')|U_{\mathbf{k}}, t', t''\rangle$. This fact is illustrated in Table I for $t' = -0.2, t'' = 0.1$. Note that $0.3 < J_c < 0.4$ for $\mathbf{k} = (\pi, 0)$, in which case we used the eigenstates for $J = 0.4$ and $J = 0.8$ to determine $|Q_{\mathbf{k}=(\pi, 0)}, t', t''\rangle$ and $|U_{\mathbf{k}=(\pi, 0)}, t', t''\rangle$. As discussed be-

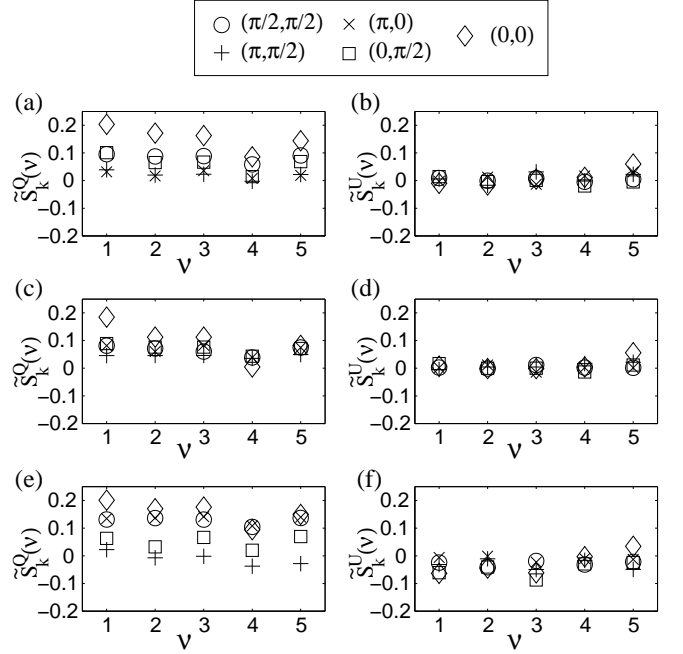


FIG. 1: Average value of the staggered magnetization on sites that are ν^{th} nearest neighbors to the hole, $\tilde{S}_{\mathbf{k}}^Q(\nu) \equiv \langle (-)^{i_x+i_y} S_{\mathbf{k}}^Q(\mathbf{i})_{\nu} \rangle$ and $\tilde{S}_{\mathbf{k}}^U(\nu) \equiv \langle (-)^{i_x+i_y} S_{\mathbf{k}}^U(\mathbf{i})_{\nu} \rangle$, for different momenta \mathbf{k} . (a) and (b) $t' = -0.3, t'' = 0.2$. (c) and (d) $t', t'' = 0$. (e) and (f) $t' = 0.3, t'' = -0.2$.

low, for $J < J_c(\mathbf{k}, t', t'')$ the eigenstate $|\psi_{\mathbf{k}}, J, t', t''\rangle$ displays properties akin to those of U states and we denote it by $|\tilde{U}_{\mathbf{k}}, J, t', t''\rangle$ (where the tilde is used to distinguish it from the U state derived for $J > J_c(\mathbf{k}, t', t'')$, which has no J dependence).

The previous argument points out that the eigenstates $|\psi_{\mathbf{k}}, J, t', t''\rangle$ have features that get enhanced by an increasing J and features that become more pronounced when J is reduced. By definition, Q and U states capture these features and, not surprisingly, below we show they display distinct physical properties: in Q states the spin antiferromagnetic (AF) order is robust to the presence of the hole while in U states the spins rearrange to facilitate hole hopping. On general grounds, a construction similar to the above one might be valid for models other than the 2D $tt't''J$ -model. The significant fact about this model is that, for experimentally relevant parameters, the overlap of both Q and U states with $|\psi_{\mathbf{k}}, J, t', t''\rangle$ is large and exhibits a considerable momentum dependence which leads to the anisotropy in k -space. [24]

Properties of Q and U states - To explore how the hole affects the spin background in Q and U states consider the spin density pattern around the hole, $S_{\mathbf{k}}^Y(\mathbf{i}) \equiv \langle Y_{\mathbf{k}} | \sum_j S_{j+i}^z \tilde{c}_{j, +1/2}^{\dagger} \tilde{c}_{j, +1/2}^{\dagger} | Y_{\mathbf{k}} \rangle + \frac{1}{N-1} \frac{1}{2}$ with $Y = Q, U$, [25] as well as the hole momentum distribution function, $n_{\mathbf{k}}^Y(\mathbf{q}, \sigma) \equiv \langle Y_{\mathbf{k}} | \tilde{c}_{-\mathbf{q}, -\sigma}^{\dagger} \tilde{c}_{-\mathbf{q}, -\sigma}^{\dagger} | Y_{\mathbf{k}} \rangle$ for $Y = Q, U$. Figs. 1(a), 1(c) and 1(e) depict the staggered magnetization in

\mathbf{k}	$t' = -0.3; t'' = 0.2$		$t' = 0.3; t'' = -0.2$	
$\mathbf{q} = (0, 0)$	0.0329	0.0343	0.0164	0.0328
$\mathbf{q} = (\pi, \pi)$	0.5437	0.6051	0.5293	0.5141

TABLE II: $\sum_{\mathbf{q}} n_{\mathbf{k}}^{\tilde{U}}(\mathbf{q}, -\frac{1}{2}) \equiv \sum_{\mathbf{q}} \langle \tilde{U}_{\mathbf{k}} | \tilde{c}_{-\mathbf{q}, \frac{1}{2}} \tilde{c}_{-\mathbf{q}, -\frac{1}{2}}^{\dagger} | \tilde{U}_{\mathbf{k}} \rangle$. $\mathbf{q} = (0, 0)$ results involve sum over $\mathbf{q} = (0, 0)$, $\mathbf{q} = (\pm\frac{\pi}{2}, 0)$ and $\mathbf{q} = (0, \pm\frac{\pi}{2})$. $\mathbf{q} = (\pi, \pi)$ results involve sum over $\mathbf{q} = (\pi, \pi)$, $\mathbf{q} = (\pm\frac{\pi}{2}, \pi)$ and $\mathbf{q} = (\pi, \pm\frac{\pi}{2})$. $J = 0.4$.

Q states, $(-)^{i_x+i_y} S_{\mathbf{k}}^Q(\mathbf{i})$, for different \mathbf{k} , t' and t'' . Since these states have a well defined quasiparticle character, the doped hole coexists with the AF spin pattern inherited from the undoped system. For the same reason, the hole momentum distribution function $n_{\mathbf{k}}^Q(\mathbf{q}, -\frac{1}{2})$ is peaked at $\mathbf{q} = \mathbf{k}$ while a smaller peak is also observed at $\mathbf{q} = \mathbf{k} + (\pi, \pi)$ due to the strong AF correlations. [26]

U states have no quasiparticle weight and display quite different behavior. Indeed, Figs. 1(b), 1(d) and 1(f) show that in $|U_{\mathbf{k}}\rangle$ the AF spin pattern of the undoped system is destroyed and the staggered magnetization around the hole [given by $(-)^{i_x+i_y} S_{\mathbf{k}}^U(\mathbf{i})$] is very close to zero and even negative. Moreover, the hole momentum distribution function $n_{\mathbf{k}}^U(\mathbf{q}, -\frac{1}{2})$ peaks around $\mathbf{q} = (\pi, \pi)$ for all momenta \mathbf{k} [Fig. 2 (a)]. The same real and momentum space properties were checked to hold for \tilde{U} states [these are the energy eigenfunctions $|\psi_{\mathbf{k}}, J, t', t''\rangle$ when $J < J_c(\mathbf{k}, t', t'')$]. This fact is illustrated for \tilde{U} states concerning the parameter regime relevant to both hole doped cuprates ($J = 0.4$, $t' = -0.3$, $t'' = 0.2$) and electron doped cuprates ($J = 0.4$, $t' = 0.3$, $t'' = -0.2$) [17] in Table II, which explicitly shows that in these states the hole density also peaks around (π, π) independently of the momenta \mathbf{k} .

According to the above spin density results the extra $S^z = -\frac{1}{2}$ spin introduced by doping spreads away from the vacancy in both U and \tilde{U} states. The resulting loss of spin exchange energy is accompanied by a gain in hole kinetic energy. Indeed, the hole momentum distribution results support that, in these states, the hole always lies around the bare band bottom [which is located at (π, π)]. This evidence resembles predictions from spin-charge separation scenarios. Indeed, within the slave-boson formalism, the electron decays into a charged spinless holon, which condenses at (π, π) , and a chargeless spinon, which describes the delocalized spin- $\frac{1}{2}$ that carries the remaining momentum. We should remark that our calculation involves equal time properties in a small lattice and does not aim to prove the existence of true spin-charge separation. However, it supports that in U and \tilde{U} states the lattice spins screen the hole in conformity with short range aspects of spin-charge separation phenomenology.

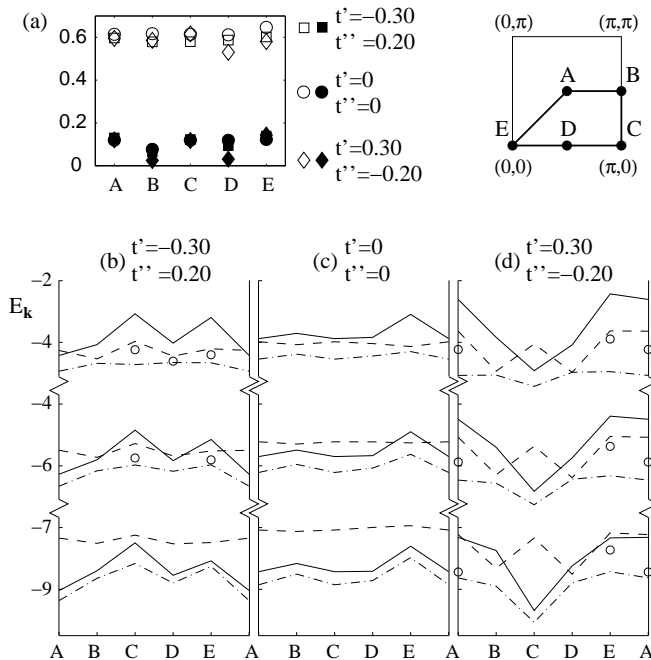


FIG. 2: (a) $\sum_{\mathbf{q}} n_{\mathbf{k}}^U(\mathbf{q}, -\frac{1}{2})$. Empty symbols involve sum over $\mathbf{q} = (\pi, \pi)$, $\mathbf{q} = (\pm\frac{\pi}{2}, \pi)$ and $\mathbf{q} = (\pi, \pm\frac{\pi}{2})$. Full symbols involve sum over $\mathbf{q} = (0, 0)$, $\mathbf{q} = (\pm\frac{\pi}{2}, 0)$ and $\mathbf{q} = (0, \pm\frac{\pi}{2})$. (b)-(d) Dispersion relations for $|Q_{\mathbf{k}}\rangle$ (full line), $|U_{\mathbf{k}}\rangle$ (dashed line) and $|\psi_{\mathbf{k}}\rangle$ (dash-dot line). Upper, middle and lower set of dispersions are obtained for J equal to 0.2, 0.4 and 0.7 respectively. (o) indicates the best energy obtained by a linear combination of $|Q_{\mathbf{k}}\rangle$ and $|U_{\mathbf{k}}\rangle$ when $J < J_c(\mathbf{k}, t', t'')$ (in which case $|\psi_{\mathbf{k}}\rangle = |\tilde{U}_{\mathbf{k}}, J, t', t''\rangle$).

t'	t''	ΔE^{ψ}	ΔE^Q	ΔE^U	$W_{\mathbf{k}'}^Q$	$W_{\mathbf{k}''}^Q$
-0.3	0.2	0.69	1.43	0.22	0	0.75
-0.2	0.1	0.56	0.92	0.14	0.45	0.72
0	0	0	0	0	0.66	0.66
0.2	-0.1	-0.75	-1.08	-0.10	0.76	0.50
0.3	-0.2	-0.80	-2.33	-0.29	0.82	0

TABLE III: ΔE^Q , ΔE^U , ΔE^{ψ} and $W_{\mathbf{k}}^Q$ with $\mathbf{k} = \mathbf{k}' \equiv (\pi, 0)$ and $\mathbf{k} = \mathbf{k}'' \equiv (\frac{\pi}{2}, \frac{\pi}{2})$ for several t' and t'' and $J = 0.4$.

The previous results demonstrate that the local configuration of spins encircling the hole is quite different in Q and U states. In this context, it is important to remark that the influence of t', t'' on the hole dispersion is sensitive to the surrounding spin environment. For instance, intrasublattice hopping is not frustrated by AF correlations and, indeed, the hole in Q states (which is surrounded by a spin configuration reminiscent of the undoped AF groundstate) strongly disperses along the AF Brillouin zone boundary (AFBZB) for $t', t'' \neq 0$ (see Fig. 2). The opposite limit occurs, for example, in certain $U(1)$ spin liquids, where the underlying spin correlations inhibit coherent intrasublattice hopping. [27] This limit

is closer to what is observed in U states, as t', t'' are heavily renormalized by the spin background (whose AF correlations are depleted by the hole nearest-neighbor hopping processes). In fact, Table III explicitly shows that $\Delta E^Q \equiv E_{(\pi,0)}^Q - E_{(\pi/2,\pi/2)}^Q$ is almost one order of magnitude larger than $\Delta E^U \equiv E_{(\pi,0)}^U - E_{(\pi/2,\pi/2)}^U$, where $E_{\mathbf{k}}^Q \equiv \langle Q_{\mathbf{k}} | H_{tt't''J} | Q_{\mathbf{k}} \rangle$ and $E_{\mathbf{k}}^U \equiv \langle U_{\mathbf{k}} | H_{tt't''J} | U_{\mathbf{k}} \rangle$.

Momentum space anisotropy - In the $tt't''J$ -model the intrasublattice hopping parameters t', t'' control the dispersion $E_{\mathbf{k}}^\psi \equiv \langle \psi_{\mathbf{k}} | H_{tt't''J} | \psi_{\mathbf{k}} \rangle$ along the AF-BZB and, thus, the pseudogap energy as well (this is the energy difference between the antinodal and nodal states $\Delta E^\psi \equiv E_{(\pi,0)}^\psi - E_{(\pi/2,\pi/2)}^\psi$). Indeed, both Fig. 2 and Table III show that these parameters set the magnitude of the pseudogap, as well as its location in k -space. [19, 28]

Interestingly t', t'' also control the difference in the quasiparticle character of $(\pi, 0)$ and $(\frac{\pi}{2}, \frac{\pi}{2})$ states, as supported by the dependence of the overlap integral $W_{\mathbf{k}}^Q \equiv |\langle \psi_{\mathbf{k}} | Q_{\mathbf{k}} \rangle|^2$ on these parameters (Table III). The resulting t', t'' driven momentum space anisotropy is particularly evident when both Q and U states have large overlaps with the eigenstates $|\psi_{\mathbf{k}}\rangle$, as it is the case for the value of J which is relevant to the cuprate systems, namely $J = 0.4$. [17, 29]

The main message of this letter is that the above roles of t', t'' can be understood with a simple two band picture involving Q and U states which captures the screening properties of the local spins encircling the hole. Indeed, as previously discussed, intrasublattice hopping is frustrated in U states and the energies $E_{(\pi,0)}^U$ and $E_{(\pi/2,\pi/2)}^U$ have a small dependence on t', t'' . In contrast, $t' < 0$ and $t'' > 0$ clearly increase the energy $E_{(\pi,0)}^Q$ and clearly decrease $E_{(\pi/2,\pi/2)}^Q$ (Fig. 2). Since $|\psi_{\mathbf{k}}\rangle$ is a superposition of $|Q_{\mathbf{k}}\rangle$ and $|U_{\mathbf{k}}\rangle$, these t', t'' induced changes in the energy of Q states push $E_{(\pi,0)}^\psi$ upward and lower $E_{(\pi/2,\pi/2)}^\psi$. Therefore, they increase the pseudogap energy ΔE^ψ . These changes also increase the energy difference $E_{(\pi,0)}^Q - E_{(\pi,0)}^U$ while reducing $E_{(\pi/2,\pi/2)}^Q - E_{(\pi/2,\pi/2)}^U$ and, as a result, $W_{(\pi,0)}^Q$ and $W_{(\pi/2,\pi/2)}^Q$ become smaller and larger respectively. For $J = 0.4, t' = -0.3, t'' = 0.2$ the energy $E_{(\pi,0)}^Q$ is so large that the minimum energy obtained by a linear combination of $|Q_{(\pi,0)}\rangle$ and $|U_{(\pi,0)}\rangle$ becomes higher than that of a different state $|\tilde{U}_{(\pi,0)}\rangle$. As a result, $W_{(\pi,0)}^Q = 0$. Since $W_{(\pi/2,\pi/2)}^Q = 0.75$, the $(\frac{\pi}{2}, \frac{\pi}{2})$ state has strong quasiparticle character and a sharp disparity between nodal and antinodal states is encountered for these parameter values. Similar behavior is obtained when $t' > 0$ and $t'' < 0$ with the role of momenta $(\pi, 0)$ and $(\frac{\pi}{2}, \frac{\pi}{2})$ interchanged (Table III).

The above argument shows that, in the pseudogap region, the kinetic energy of a hole surrounded by an AF configuration of spins increases as the pseudogap gets larger. When this kinetic energy exceeds a certain value

the spins around the hole lose their staggered pattern and, at short distances, the doped spin and charge separate. The resulting nodal-antinodal dichotomy, found to occur in the parameter regimes concerning hole and electron doped cuprates, follows from local energetic considerations and not from the interaction of holes with other holes, an incipient order parameter or disorder. It also agrees with previous numerical evidence for spin-charge separation phenomenology at high energy. [15, 16]

Following our results, a new mean field theory of the $tt't''J$ -model was recently proposed that describes holes dressed by two different spin configurations. [30] It accounts for the observed momentum space anisotropy and is in good agreement with the doping dependence of ARPES experiments.

The author is grateful to X.-G. Wen and P.A. Lee for discussions and valuable comments on the manuscript. This work was partially supported by the Fundação Calouste Gulbenkian Grant No. 58119 (Portugal), NFSC Grant No. 10228408 (China), NSF Grant No. DMR-01-23156 and NSF-MRSEC Grant No. DMR-02-13282.

-
- [1] O. Parcollet *et al.*, Phys. Rev. Lett. **92**, 226402 (2004).
 - [2] X.J. Zhou *et al.*, Phys. Rev. Lett. **92**, 187001 (2004).
 - [3] A. Damascelli *et al.*, Rev. Mod. Phys. **75**, 473 (2003).
 - [4] T. Yoshida *et al.*, Phys. Rev. Lett. **91**, 027001 (2003).
 - [5] F. Ronning *et al.*, Phys. Rev. B **67**, 165101 (2003).
 - [6] A. Kaminski *et al.*, Phys. Rev. B **71**, 014517 (2005).
 - [7] K. McElroy *et al.*, cond-mat/0406491.
 - [8] D. van der Marel, Phys. Rev. B **60**, R765 (1999).
 - [9] S. Ono and Y. Ando, Phys. Rev. B **67**, 104512 (2003).
 - [10] N.P. Armitage *et al.*, Phys. Rev. Lett. **88**, 257001 (2002).
 - [11] A. Koitzsch *et al.*, Phys. Rev. B **67**, 184522 (2003).
 - [12] R.W. Hill *et al.*, Nature **414**, 711 (2001).
 - [13] T. Hanaguri *et al.*, Nature **430**, 1001 (2004).
 - [14] L.B. Ioffe and A.J. Millis, Phys. Rev. B **58**, 11631 (1998).
 - [15] T. Tohyama *et al.*, J. Phys. Soc. Jpn. **69**, 9 (2000).
 - [16] W.-C. Lee *et al.*, Phys. Rev. Lett. **91**, 057001 (2003).
 - [17] T. Tohyama and S. Maekawa, Supercond. Sci. Technol. **13**, R17 (2000).
 - [18] G.B. Martins *et al.*, Phys. Rev. B **60**, R3716 (1999).
 - [19] T. Tohyama, Phys. Rev. B **70**, 174517 (2004).
 - [20] G. Martinez and P. Horsch, Phys. Rev. B **44**, 317 (1991).
 - [21] S. Schmitt-Rink *et al.*, Phys. Rev. Lett. **60**, 2793 (1988).
 - [22] A. Ramšak and P. Horsch, Phys. Rev. B **57**, 4308 (1998).
 - [23] Any two values of $J \in [0.2, 0.8]$ other than $J = 0.2, 0.6$ lead to practically the same $|Q_{\mathbf{k}}\rangle$ and $|U_{\mathbf{k}}\rangle$.
 - [24] We expect that U states derived for the 3D $tt't''J$ -model be of less relevance than those obtained for the 2D model since AF correlations are more robust in 3D.
 - [25] To reduce finite size effects we subtract the average magnetization $\frac{1}{N-1} \sum_j \langle S_j^z \rangle = -\frac{1}{N-1} \frac{1}{2}$, where N is the number of lattice sites.
 - [26] R. Eder and Y. Ohta, Phys. Rev. B **51**, 6041 (1995).
 - [27] T.C. Ribeiro and X.-G. Wen, Phys. Rev. B **68**, 024501 (2003).
 - [28] K. Tanaka *et al.*, Phys. Rev. B **70**, 092503 (2004).

- [29] J increases the robustness of the AF background thus enhancing the quasiparticle behavior. Hence, larger values of J decrease the weight of U states.
- [30] T.C. Ribeiro and X.-G. Wen, cond-mat/0410750.